Microbial Pathogenesis 203 (2025) 107488

Contents lists available at ScienceDirect

Microbial Pathogenesis

journal homepage: www.elsevier.com/locate/micpath

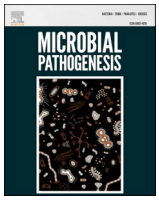

Isolation and characterization a novel *Acinetobacter* bacteriophage with activity against several multidrug-resistant Gram-negative bacteria

Yelda İşlek [a,b], Nur Hamzeli [a,c], Ahmet Aktaş [a,d,*], Fatma Köksal Çakırlar [a]

[a] Department of Medical Microbiology, Cerrahpaşa Faculty of Medicine, İstanbul University-Cerrahpaşa, İstanbul, Türkiye
[b] Vocational College, Kapadokya University, Nevşehir, Türkiye
[c] Turkish Red Crescent, Northern Marmara Regional Blood Center, İstanbul, Türkiye
[d] İstanbul Provincial Health Directorate, İstanbul Public Health Laboratory No. 2, İstanbul, Türkiye

ARTICLE INFO

Keywords:
Acinetobacter baumannii
Bacteriophage
Endolysin
Obolenskvirus
Multidrug resistance
Holin

ABSTRACT

Acinetobacter baumannii (A. baumannii) is a notorious nosocomial pathogen that is frequently associated with multidrug resistance around the world. Endolysin is a bacteriophage-produced hydrolytic enzyme. In this study, an urban waste water sample (1 L) was collected from Istanbul. A double-agar plating technique was used for host range analysis. The purified genomic DNA sequences were performed on the Miseq. De novo assembly of the crude sequences yielded a double-stranded DNA molecule with a length of 45,679 bp and a guanine-cytosine content of 37.6%. Genome annotation revealed that the vB_AbaM_YNAF genome comprises 85 open reading frames, 23 of which are functional and do not define any tRNA-rRNA genes. Electron microscopy examination and phylogenetic analysis of the genome revealed that vB_AbaM_YNAF represents a novel origin of an unclassified *Obolenskvirus* belonging to the class *Caudoviricetes*. vB_AbaM_YNAF infected one reference and three different multidrug-resistant (MDR) strains of each of *A. baumannii* and *K. pneumoniae*. However, it did not have any effect on a reference *E. coli* strain. Based on all of these findings, LysYAN could be a potential agent for treating MDR-Gram-negative bacteria. Further investigations on vB_AbaM_YNAF may be beneficial for designing an alternative weapon with probable wide host-range activity to fight MDR infections.

1. Introduction

Acinetobacter spp. is a Gram-negative bacterium that is non-fermentative, opportunistic, and common in the environment. *Acinetobacter baumannii* (*A. baumannii*) is responsible for approximately 90 % of clinical infections of all *Acinetobacter* spp. in humans [1]. Its ability to survive harsh conditions, including drying and disinfection, allows it to persist and spread in hospital settings. In addition to *A. baumannii*'s natural resistance to many antibiotics, including cephalosporins, this pathogen can also acquire resistance to other antibiotics. Efflux pump overexpression, reduced permeability, and hydrolytic enzyme production are examples of the acquired resistance mechanisms identified in *A. baumannii* [2].

The mortality rate of *A. baumannii* infections is high, and nosocomial outbreaks with multidrug-resistant (MDR) *A. baumannii* have been frequently reported worldwide [3]. In 2017, the World Health Organization (WHO) published a list of "priority pathogens" that are resistant to antibiotics, consisting of 12 bacterial families that pose the greatest threat to human health. The WHO list is divided into three categories: critical, high, and medium priority, based on the urgency of the need for new antibiotics. The most critical group includes multidrug-resistant bacteria, which pose a particular threat in hospitals, nursing homes, and among patients who require devices such as ventilators and blood catheters for their care. These include *Acinetobacter, Pseudomonas*, and *Enterobacteriaceae* [4].

Bacteriophages, also called phages, are viruses that are pathogenic only to bacteria and are able to control the biosynthetic mechanism of the bacterial host, enabling them to produce different viral proteins. Phages are primitive organisms containing nucleic acids (DNA or RNA) that encode the information necessary for their replication outside the host cell and are found in various environments, such as soil, water, and feces [5].

Phages were discovered by Felix d'Herelle in 1917. Following his discovery, he suggested that phages could be used as a therapeutic tool. He successfully treated *Shigella* dysentery patients in France and a cholera epidemic in India with phage preparations. Since then, phage

* Correspondance Author. Kocamustafapaşa st. 34098, Fatih, İstanbul, Türkiyeahmet.aktas@ymail.com
E-mail addresses: yelda.islek@kapadokya.edu.tr (Y. İşlek), nurhamzeli@gmail.com (N. Hamzeli), fatma.koksal@istanbul.edu.tr (F. Köksal Çakırlar).

https://doi.org/10.1016/j.micpath.2025.107488
Received 14 October 2024; Received in revised form 27 February 2025; Accepted 14 March 2025
Available online 14 March 2025

therapy has been recognized as an important therapeutic tool and a specific treatment for bacterial infections [6]. Typically, bacteriophage morphology exhibits a well-defined three-dimensional structure. The genetic material is surrounded by an icosahedral protein capsid head, a tail (spiral contractile sheath surrounding a nuclear tube and a base plate with tail fibers), and surface receptor proteins responsible for recognizing specific surface molecules on the host bacteria [7].

Phages can multiply in bacterial cells through two strategies: lytic and lysogenic. Lytic phages insert their genome into the host cell's cytoplasm and produce proteins using bacterial ribosomes, causing the cell's death through either active or passive lysis. On the other hand, the genomes of lysogenic phages can either be inserted into the cytoplasm as a circular replicon or integrated into the bacterial chromosome [8]. In this study, a new *A. baumannii*-specific lytic phage was identified, and its activity was investigated on various Gram-negative bacteria.

2. Materials and methods

2.1. Phage isolation and purification

An urban wastewater sample (1 L) was collected from Istanbul. Then 15 mL of distilled water was added to 35 mL of waste water sample and vortexed. The mixture was then centrifuged at 5000 rpm for 15 min, after which the supernatant was passed through a 0.22 μm pore diameter filter and placed in a sterile tube. From the culture collection, 1 mL of suspension of MDR *A. baumannii* ST2 (10^8 cfu/mL) and 10 mL of TBS were added to the supernatant, mixed, and incubated in an oven at 120 rpm and 37 °C with shaking for 18 h. At the end of the incubation period, the sample was centrifuged again at 5000 rpm for 15 min. The supernatant was filtered twice through a 0.22 μm pore diameter filter and stored at 4 °C without the chloroform step described in Merabishvili's study [9].

2.2. Host range analysis

A double-agar plating technique was used for host range analysis. A 100-μL (10^8 cfu/mL) suspension of MDR *A. baumannii* ST2 was added to 5 mL of TSA containing 0.4% agar, mixed, and spread homogeneously on plates containing TSA. The plates were then frozen for 15 min. A 15 μL suspension of phage (10^9 pfu/mL) was then added to the plate, dried at room temperature, and incubated at 37 °C for 18 h. These procedures were repeated for *Klebsiella pneumoniae* (*K. pneumoniae*) ATCC 700600, *Escherichia coli* (*E. coli*) ATCC 25992, *A. baumannii* ATCC 19606 reference strains as well as MDR *A. baumannii* (n = 10) and MDR *K. pneumoniae* (n = 10).

2.3. Determination of multiplicity of infection (MOI)

The multiplicity of infection (MOI) of phage vB_AbaM_YNAF was determined according to the methods previously outlined in Ref. [10]. In summary, 100 μL of *A. baumanni* (OD_{600} = 0.4, 10^8 cfu/mL) and 100 μL of phage vB_AbaM_YNAF were added to 900 μL of TSB, yielding phage-to-bacteria ratios, of 0.01, 0.1, 1, and 10. The mixture was then subjected to an incubation period at a temperature of 37 °C for 6 h. Thereafter, the phage and bacterial titers were determined using double-layer plating.

2.4. Detection of physicochemical stability

Detection of phage temperature and pH stability involved 100 μL phage suspension (10^9 pfu/mL) incubated at 4, 37, 50, and 85 °C for 1 h. The phage suspension was incubated at various pH values (pH 2, 4, 7, 10, and 12) for 1 h at room temperature to assess the pH stability of the phage. The phage titer was determined using the double-layer plate technique [11].

2.5. One-step growth curve

The one-step growth curve of the isolated phage was conducted as in the previous study [12]. Briefly, the isolated phage was introduced to *A. baumannii* and *K. pneumoniae* at a MOI of 10 and allowed to adsorb for 15 min at 37 °C. The mixture was subsequently centrifuged at 10,000×*g* for 1 min to remove non-adsorbed phages. The resulting pellet, containing phage-infected bacterial cells, was resuspended in fresh LB broth and incubated under shaking conditions at 180 rpm and 37 °C. Aliquots were collected at 5-min intervals, and phage titers were immediately quantified using the double-layer agar method. The latent period was determined directly from the one-step growth curve, while the burst size was calculated by dividing the total number of phages produced during the rise period by the estimated number of infected cells at the onset of the latent period [13].

2.6. Viral DNA sequencing and genome analysis

Viral DNA was isolated with the Illumina DNA Prep DNA isolation kit. The amount of DNA was measured with Qubit 2.0 (Thermo Fisher, USA) and adjusted according to the values specified in the kit (280/260: ~1.80). The nM values of the samples were calculated with the following equation: nM = ng/μL*10^6/(656.6*1200). Adapters and libraries were prepared as specified in the Nextera DNA CD Index's procedure (Illumina, USA). The purified genomic DNA sequences were performed on the Miseq platform using the Nexera DNA Library (Illumina, USA). After quality control of the chains obtained from sequencing was performed with FastQC, the raw sequences were assembled de novo using the SPAdes v3.15.5. Each open reading frame (ORF) was annotated using Prokka v1.14.6 and Phigaro v1.0.1. A second round of annotation was subsequently executed following the initial annotation in order to confirm or modify protein function assignments using the NCBI BLASTp. The presence of transfer RNA (tRNA)-coding regions was investigated using the tRNAscan-SE v2.0.12. Antibiotic resistance genes were investigated using ncbi-AMRFinderplus v3.12.8. Mauve was used for genome comparison. A heat map was prepared with associated phages using the VIRIDIC pipeline. The phylogenetic tree was constructed using the neighbor-joining method in Mega v11 and visualized with the iTOL v6 command-line tool.

2.7. Transmission electron microscopy (TEM)

Transmission electron microscope (TEM) imaging was performed as described in previous work [14]. A 10-μL sample of the phage, with a concentration of 10^9 pfu/mL, was stained with 2.5% uranyl acetate. The sample was then placed on a carbon-coated copper grid and left to dry for 10 min before being examined using a TEM. Images of the stained phage were taken at various magnifications using the TEM (Jeol JEM 1010, Japan).

2.8. Statistical analysis

The statistical analyses of the data obtained from physicochemical analysis studies were performed using SPSS v26. The normality of the data was assessed with the Shapiro-Wilk test, while variance homogeneity was evaluated using Levene's test. The comparison of means between groups (*A. baumannii* vs. *K. pneumoniae*) was conducted using the independent samples *t*-test.

3. Results

3.1. Host range results

To investigate the role of various Gram-negative bacteria in phage infectivity, we assessed the ability of vB_AbaM_YNAF to infect a range of bacterial strains at a titer of 1.5 × 10^8 pfu/mL. Clinical isolates of MDR

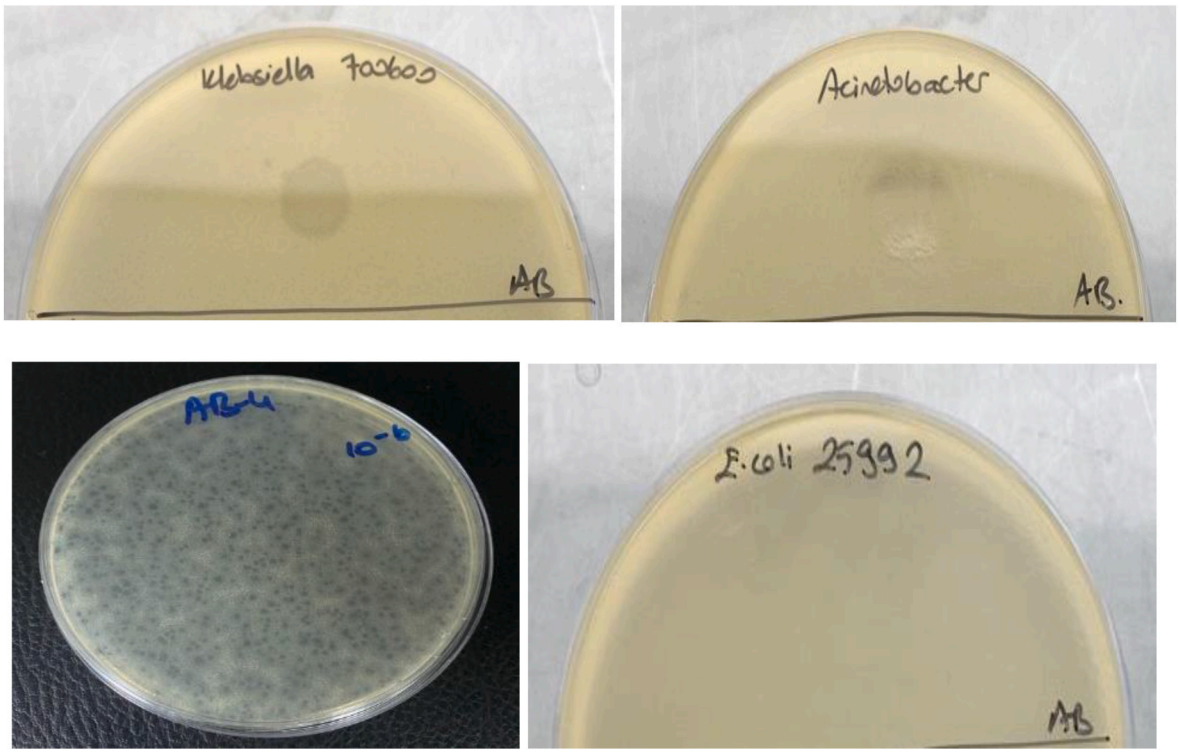

Fig. 1. Spot test and host range analysis results of vB_AbaM_YNAF.

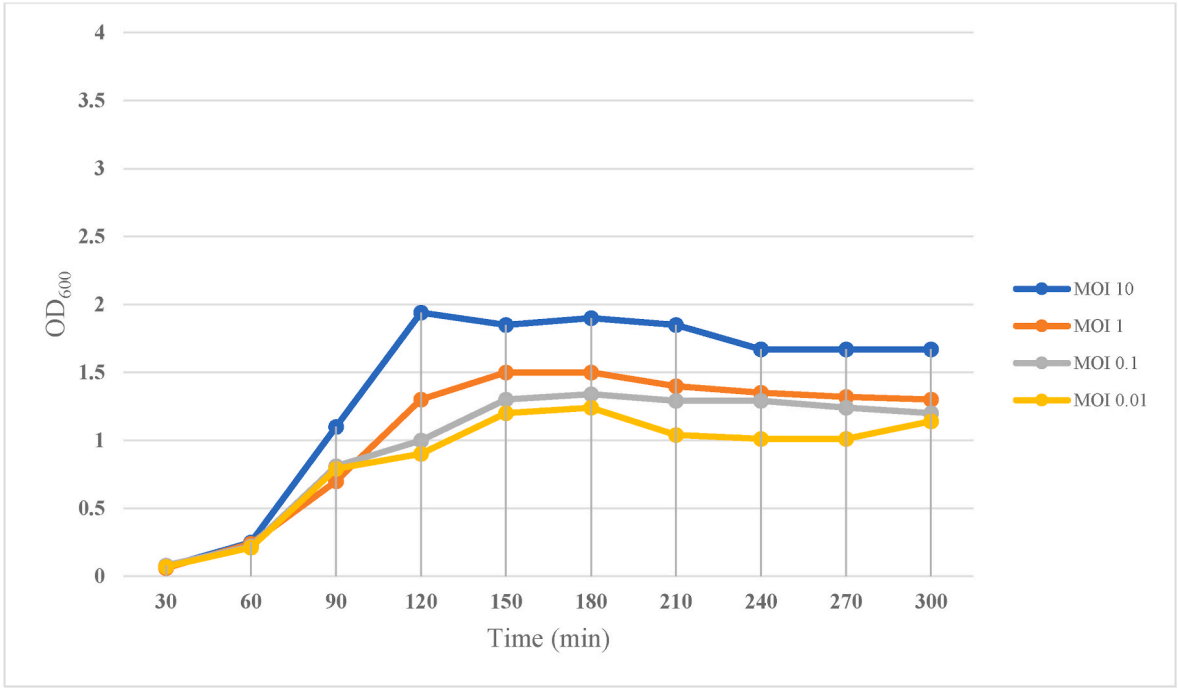

Fig. 2. The reduction in growth of MDR *A. baumannii* by phage vB_AbaM_YNAF at various MOIs.

A. baumannii (n = 10) and MDR *K. pneumoniae* (n = 10) along with the reference strain *E. coli* ATCC 25992, were tested. The results demonstrated that vB_AbaM_YNAF was capable of infecting all bacterial isolates except for *E. coli* (Fig. 1).

3.2. MOI results

The activity of phage vB_AbaM_YNAF against different MDR *A. baumannii* strains varied depending on the applied MOI values. The MOI values for the strains used in this study ranged from 0.055 to 1.5 for *A. baumannii* strains. Notably, higher MOI values resulted in faster and more efficient lytic activity. However, at lower MOI values, a noticeable

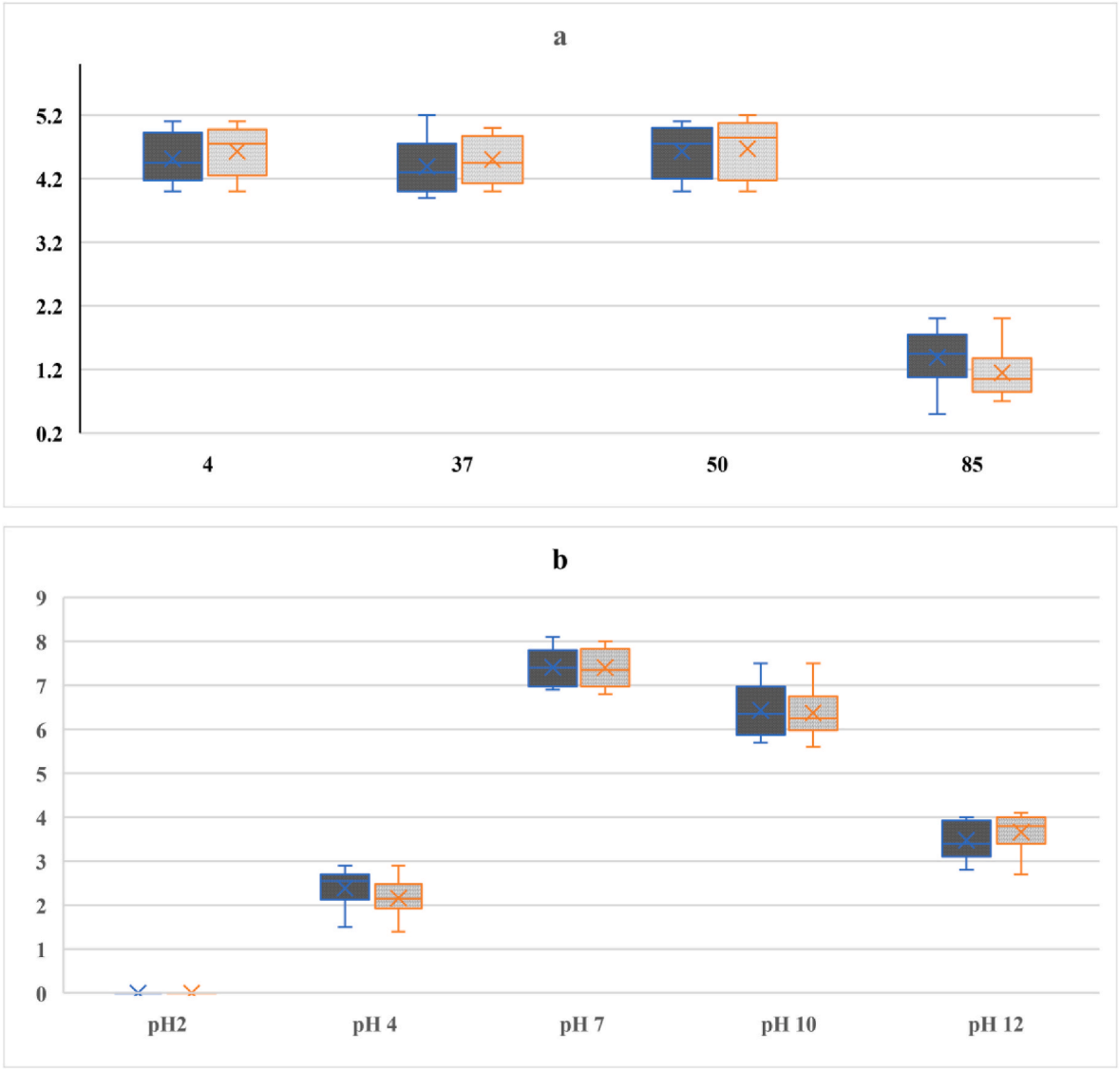

Fig. 3. Stability of vB_AbaM_YNAF under different conditions. (**a**) Thermal stability of vB_AbaM_YNAF incubated at different temperatures for 1 h. Vertical bar phage titer $\log_{10}$ (pfu/mL); Horizontal bar temperature (°C); (**b**) pH stability of vB_AbaM_YNAF incubated at different pHs for 1 h. Vertical bar phage titer $\log_{10}$ (pfu/mL); Horizontal bar pH. Left: *A. baumannii*, Right: *K. pneumoniae*.

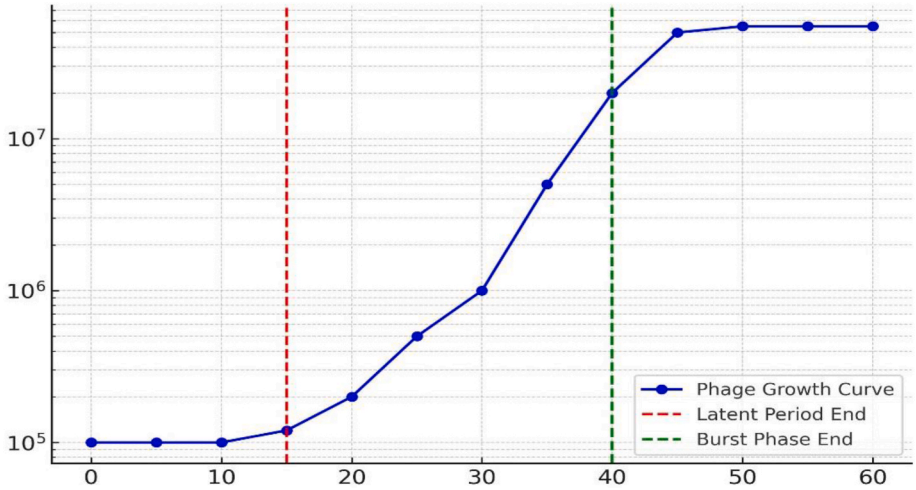

Fig. 4. One-Step Growth Curve of phage vB_AbaM_YNAF. Vertical bar phage titer (pfu/mL); Horizontal bar time (min).

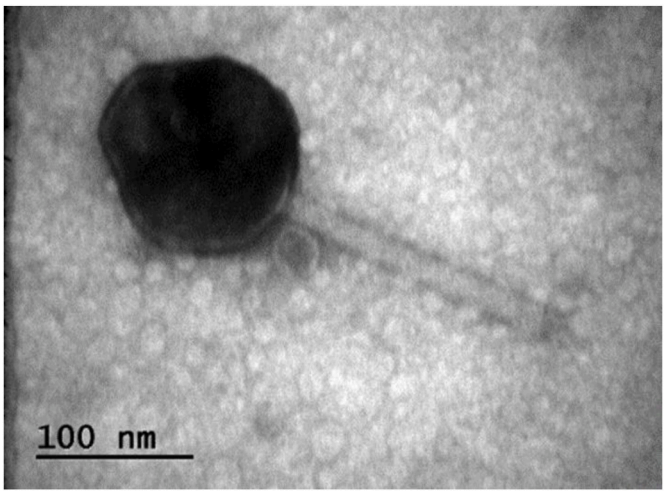

Fig. 5. Transmission electron microscope image of vB_AbaM_YNAF.

reduction in phage activity was observed (Fig. 2). These results highlight the significant impact of MOI on phage efficacy, demonstrating that higher MOI values provide greater efficiency, particularly in more densely populated bacterial cultures.

3.3. Physicochemical stability of vB_AbaB_YNAF

Phage stability is a crucial determinant of its efficacy, as both pH and temperature significantly influence its structural integrity and lytic activity. Heat stability assays at 4 °C, 37 °C, 50 °C, and 85 °C showed a significant reduction in the activity of phage vB_AbaM_YNAF against *A. baumannii* and *K. pneumoniae* after 1 h at 85 °C (p-values: 0.00011 and 0.00013, respectively) compared to 50 °C. In contrast, no significant activity loss was observed at lower temperatures (37 °C: $p = 0.558$, 50 °C: $p = 0.841$), indicating thermal resilience under these conditions (Fig. 3a). No statistically significant differences were found between *A. baumannii* and *K. pneumoniae* at any tested temperature.

pH stability analysis revealed complete inactivation at pH 2, likely due to protein denaturation. The phage maintained its activity at pH 4, 7, 10, and 12, with optimal stability and lytic performance observed at pH 7, indicating a preference for neutral conditions. However, its activity significantly decreased at pH 4 and 12 against *A. baumannii* (pH 4 vs. pH 7, $p = 0.00474$; pH 10 vs. pH 12, $p = 0.00012$) and *K. pneumoniae* (pH 4 vs. pH 7, $p = 0.00012$; pH 10 vs. pH 12, $p = 0.00011$). This reduction suggests a loss of phage functionality under acidic and alkaline conditions. (Fig. 3b).

3.4. Phage one-step growth curve results

The one-step growth curve of the isolated bacteriophage was characterized by three distinct phases: latency, burst, and plateau. The latency period lasted approximately 15 min. A rapid increase and

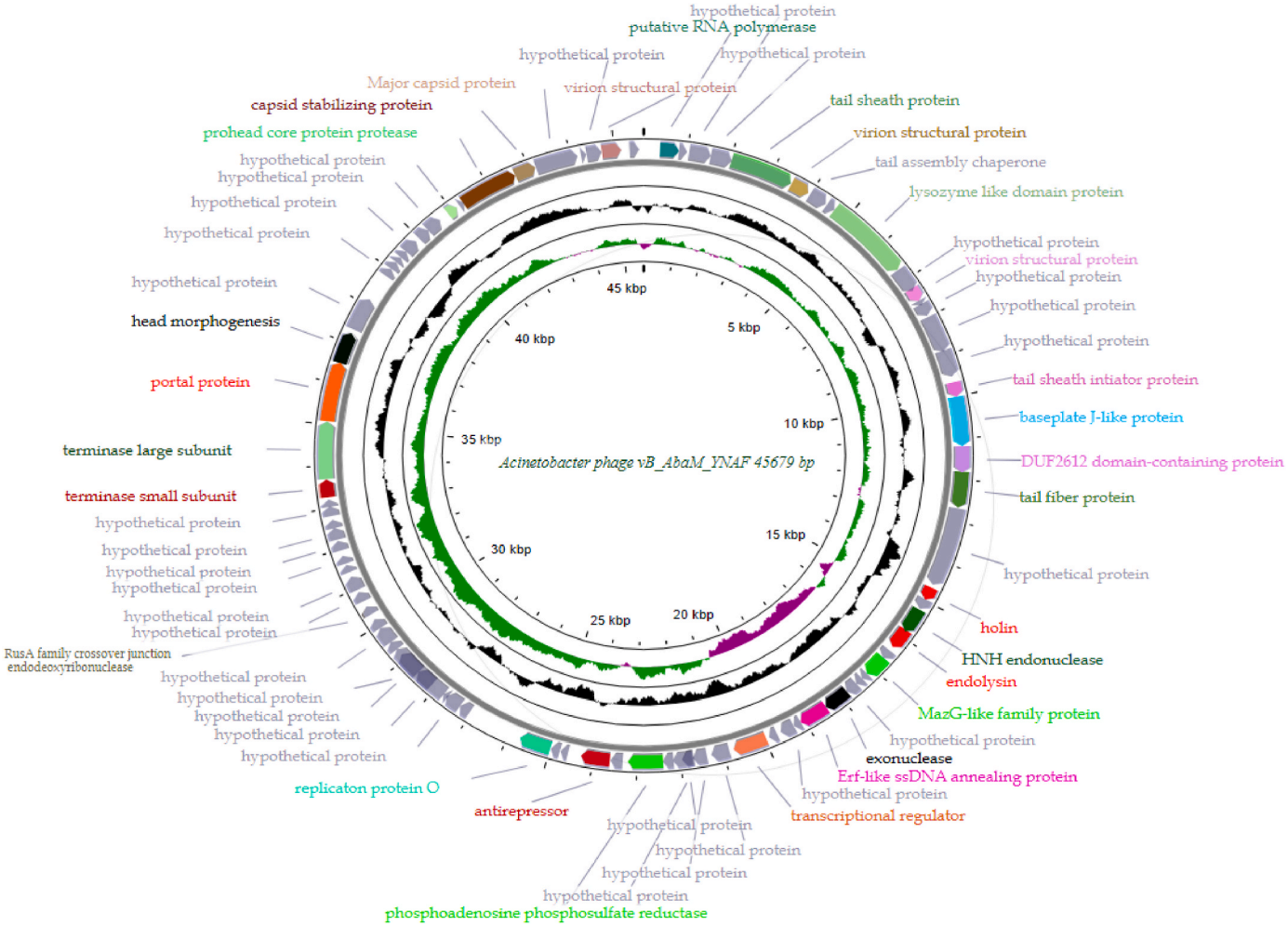

Fig. 6. Circular genome and protein map of vB_AbaM_YNAF.

Table 1
Functional ORFs list of vB-AbaM_YNAF.

Name	Start	Stop	Direction	locus_tag	Protein ID
Putative RNA polymerase	375	812	forward	yan_1	WYA82678
Tail steath protein	2025	3488	forward	yan_5	WYA82682
Virion structural protein	3501	3950	forward	yan_6	WYA82683
Tail assembly chaperone	3996	4421	forward	yan_7	WYA82684
Lysozyme-like domain protein	4666	6696	forward	yan_9	WYA82686
Virion structural protein	7239	7580	forward	yan_11	WYA82688
Tail sheath initiator protein	9669	10022	forward	yan_16	WYA82693
Baseplate J-like protein	10019	11203	forward	yan_17	WYA82694
DUF2612 domain-containing protein	11203	11829	forward	yan_18	WYA82695
Tail fiber protein	11807	12667	forward	yan_19	WYA82696
Holin	14662	14982	forward	yan_21	WYA82698
HNH endonuclease	15249	15860	reverse	yan_23	WYA82700
Endolysin	15822	16334	forward	yan_24	WYA82701
MazG-like family protein	16656	17189	reverse	yan_26	WYA82703
Exonuclease	17819	18385	reverse	yan_29	WYA82706
Erf-like ssdna annealing protein	18418	19098	reverse	yan_30	WYA82707
Transcriptional regulator	19972	20763	reverse	yan_34	WYA82711
Phosphoadenosine phosphosulfate reductase	22402	23202	forward	yan_40	WYA82717
Antirepressor	23617	24285	forward	yan_42	WYA82719
Replication protein O	25008	25742	forward	yan_45	WYA82722
Replicative DNA helicase	25727	27043	forward	yan_46	WYA82723
Nucleotide kinase	29284	29511	forward	yan_53	WYA82730
RusA family endodeoxyribonuclease	30300	30521	forward	yan_56	WYA82733
Terminase small subunit	33264	33701	forward	yan_65	WYA82742
Terminase large subunit	33701	35074	forward	yan_66	WYA82743
Portal protein	35077	36507	forward	yan_67	WYA82744
Head morphogenesis protein	36510	37280	forward	yan_68	WYA82745
Prohead core protein protease	41300	42661	forward	yan_79	WYA82756
Capsid stabilizing protein	42661	43155	forward	yan_80	WYA82757
Major capsid protein	43166	44158	forward	yan_81	WYA82758
Virion structural protein	44720	45172	forward	yan_84	WYA82761

oscillation in phage titer were observed between 15 and 40 min, indicating efficient replication. After 40 min, the depletion of host bacterial cells resulted in the stabilization of phage concentration. These findings suggest that phage vB_AbaM_YNAF exhibits a short latency period and a high burst size, demonstrating strong infectivity and significant antimicrobial potential against *A. baumannii* and *K. pneumoniae* (Fig. 4).

3.5. Genome analysis results

In this study, we isolated and characterized an *Acinetobacter* phage vB_AbaM_YNAF from urban waste water in Istanbul (Fig. 5). De novo assembly of the crude sequences yielded a double-stranded DNA molecule with a length of 45,679 base pairs and a guanine-cytosine (GC) content of 37.6%. Genome annotation revealed that the vB_AbaM_YNAF genome comprises 85 open reading frames (ORFs), 23 of which are functional and do not define any tRNA-rRNA genes and antibiotic resistance genes (Fig. 6). These can be categorized into four groups according to function, including lysis, structure, transcription/translation, and undefined function (Table 1). Phylogenetic analysis of the genome revealed that vB_AbaM_YNAF represents a novel origin of an unclassified *Obolenskvirus* belonging to the class *Caudoviricetes* (Fig. 7). The genome data have been deposited in Genbank under accession number PP355976.

A blast analysis revealed that vB_AbaM_YNAF exhibited limited similarities with other *Acinetobacter*-specific phage genomes included in the databases. Furthermore, no similarity was observed with phages specific for other Gram-negative bacteria, including *E. coli* and *K. pneumoniae* (Fig. 8).

The top five most similar sequences were identified as *Acinetobacter* phage Ab59 (total score: 54916, coverage: 74%, OR045357.1), *Acinetobacter* phage Ab65 (total score: 54921, coverage: 74%, OR045358.1), *Acinetobacter* phage Ab31 (total score: 54899, scope: 74%, OR045355.1), *Acinetobacter* phage vB_AbaM_IME512 (total score: 53113, scope: 78%, MH853788.1), and *Acinetobacter* phage P1068 (total score: 49991, scope: 75%, OQ689089.1) (Fig. 9).

The major capsid protein of vB_AbaM_YNAF (yan_81) exhibited a high degree of similarity to *Acinetobacter* phage Ab31 (maximum score: 677, 100% identical), *Acinetobacter* phage BUCT629 (maximum score: 675), *Acinetobacter* phage HZY2308 (maximum score: 674), and *Acinetobacter* phage AB1 (maximum score: 673)

The amino acid sequence of the terminase large subunit (yan_66) involved in the packaging of genetic material includes *Acinetobacter* phage Ab31 (max. score: 944, 100% ident), *Acinetobacter* phage Cato (max. score: 943, 99.78% ident), *Acinetobacter* phage vB_AbaM_IME512 (max. score: 939, 99.34% ident), and *Acinetobacter* phage LZ35 (max. score: 937, 98.69% ident). The small subunit (yan_65) amino acid sequence exhibited a high degree of similarity to *Acinetobacter* phage Cato (max. score: 304, 100% ident), *Acinetobacter* phage AbP2 (max. score: 298, 98.6% ident), and *Acinetobacter* phage LZ35 (max. score: 243, 78.62% ident).

The MazG protein of vB_AbaM_YNAF (yan_26) exhibited a high degree of similarity to *Acinetobacter* phage vB_AbaM_AB3P2 (max. score: 353, 97.18% identity), *Acinetobacter* phage WCHABP12 (max. score: 344, 91.53% identity), and *Acinetobacter* phage vB_AbaM-IME-AB2 (max. score: 208, 61.41% identity). The Capsid Stabilizing Protein (yan_80) of vB_AbaM_YNAF exhibited a high degree of similarity to *Acinetobacter* phage Scipio (max. score: 327, 100% identity), *Acinetobacter* phage Ab31 (max. score: 325, 100% identity), and *Acinetobacter* phage Cato (max. score: 178, 99% identity).

Acinetobacter phage WCHABP1, *Acinetobacter* phage vB_AbaM-fThrA, *Acinetobacter* phage LZ35, and *Acinetobacter* phage vB_AbaM-IME-AB2 were found to share an amount of amino acid sequence similarity with the endolysin of vB_AbaM_YNAF (LysYAN). With a rating of 95.8%, the WCHABP1 endolysin was found to be the most similar to the other endolysins. The sequence alignment study showed that the vB_AbaM_YNAF endolysin is three amino acids longer than the WCHABP1 endolysin and contains seven amino acids (D60E, T110K, A111D, S125A, Q126I, D130E, and K134R) (Fig. 10).

The holin of vB_AmaB_YNAF (yan_21) exhibited the similarity to *Acinetobacter* phage Cato (max score: 205, 99.06% ident, e-value: 1e-

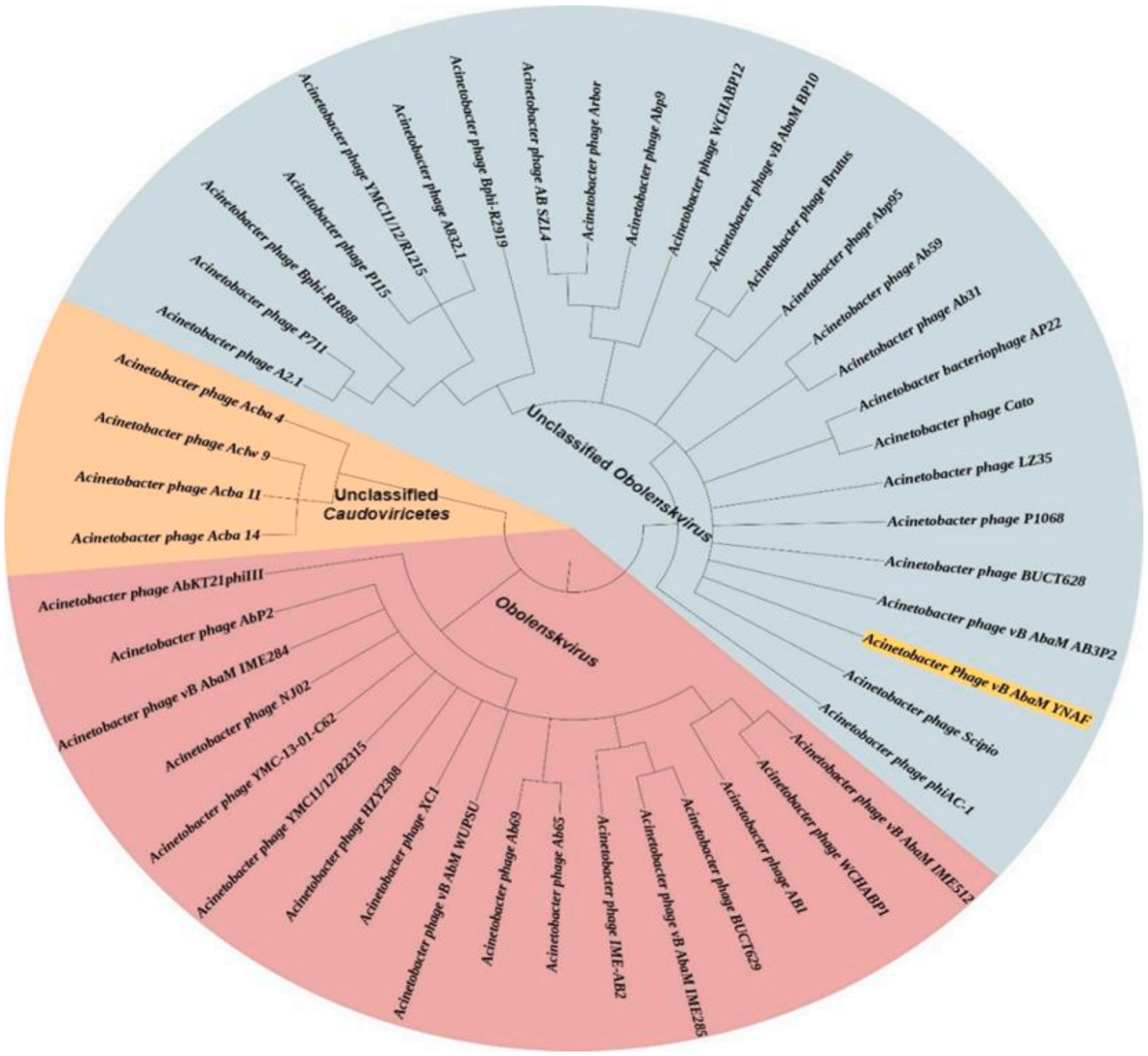

Fig. 7. Phylogenetic tree showing relatedness of vB_AbaM_YNAF to the *Caudoviricetes*.

66), *Acinetobacter* phage Scipio (max score: 205, 98.11% ident, e-value: 3e-66), and *Acinetobacter* phage Brutus (max score: 205, 98.11 % ident, e-value: 4e-66) (Fig. 11).

vB_AbaM_YNAF, like other members of the *Obolenskvirus*, was found to have a region (yan_9) encoding a lysozyme-like protein. This peptide sequence of 676 amino acids was similar to *Acinetobacter* phage WCHABP12 (max score: 1337, 96.15% ident) and *Acinetobacter* phage AP22 (max score: 1335, 96.15% ident) and *Acinetobacter* phage WCHABP1 (max score: 1297, 95.12% ident).

4. Discussion

Infections with MDR bacteria are one of the world's leading public health threats, with high mortality rates and significant economic burdens. The majority of reported MDR infections are of nosocomial origin. A group of Gram-positive and Gram-negative bacteria (*Enterococcus faecium, Staphylococcus aureus, K. pneumoniae, A. baumannii, Pseudomonas aeruginosa*, and *Enterobacter* spp.) considered the major nosocomial pathogens are defined by the 'ESKAPE' acronym [15].

In this study, we isolated and characterized a novel *Acinetobacter* phage, vB_AbaM_YNAF, which exhibited antimicrobial activity against various Gram-negative bacteria, including MDR *A. baumannii*, *K. pneumoniae*. Tailed phages with double-stranded DNA are classified within the order *Caudoviricetes*, which comprises three taxa: *Siphoviridae*, *Myoviridae*, and *Podoviridae*. These taxa are distinguished by their virion morphology [16]. Phylogenetic analyses revealed that vB_AbaM_YNAF is a novel virus related to the previously identified but unclassified *Obolenskviruses* in the *Caudoviricetes* class of tailed viruses. Nevertheless, while sharing de facto common family features, phage vB_AbaM_YNAF exhibited a markedly different DNA sequence similarity profile when compared to other phages of the *Obolenskvirus*.

Tailed phages utilize a terminase mechanism consisting of large and small subunits to package the genome and load it into the capsid. While the small subunit is involved in initiating DNA synthesis, the large subunit is involved in stopping synthesis and packaging new DNA when sufficient amounts are present [17,18]. Therefore, these two critically important proteins are one of the cornerstones of phylogenetic analyses [19]. In a comparison of NCBI data, although the terminase large subunit of vB_AbaM_YNAF was similar to the terminase large subunit of *Acinetobacter* phage Ab1, the small subunit was not phylogenetically close. This supports the idea that other encoded proteins are also effective in establishing phylogenetic distances.

MazG domain-containing proteins aid to extend the logarithmic phase of bacterial growth by starting up metabolic pathways that were turned off when the bacteria did not have enough food [20]. The MazG protein was encoded only as *Acinetobacter* phage WCHABP1 and *Acinetobacter* phage WCHABP12. The MazG blast results showed that WCHABP12 had the highest similarity to vB_AbaM_YNAFs (yan_26).

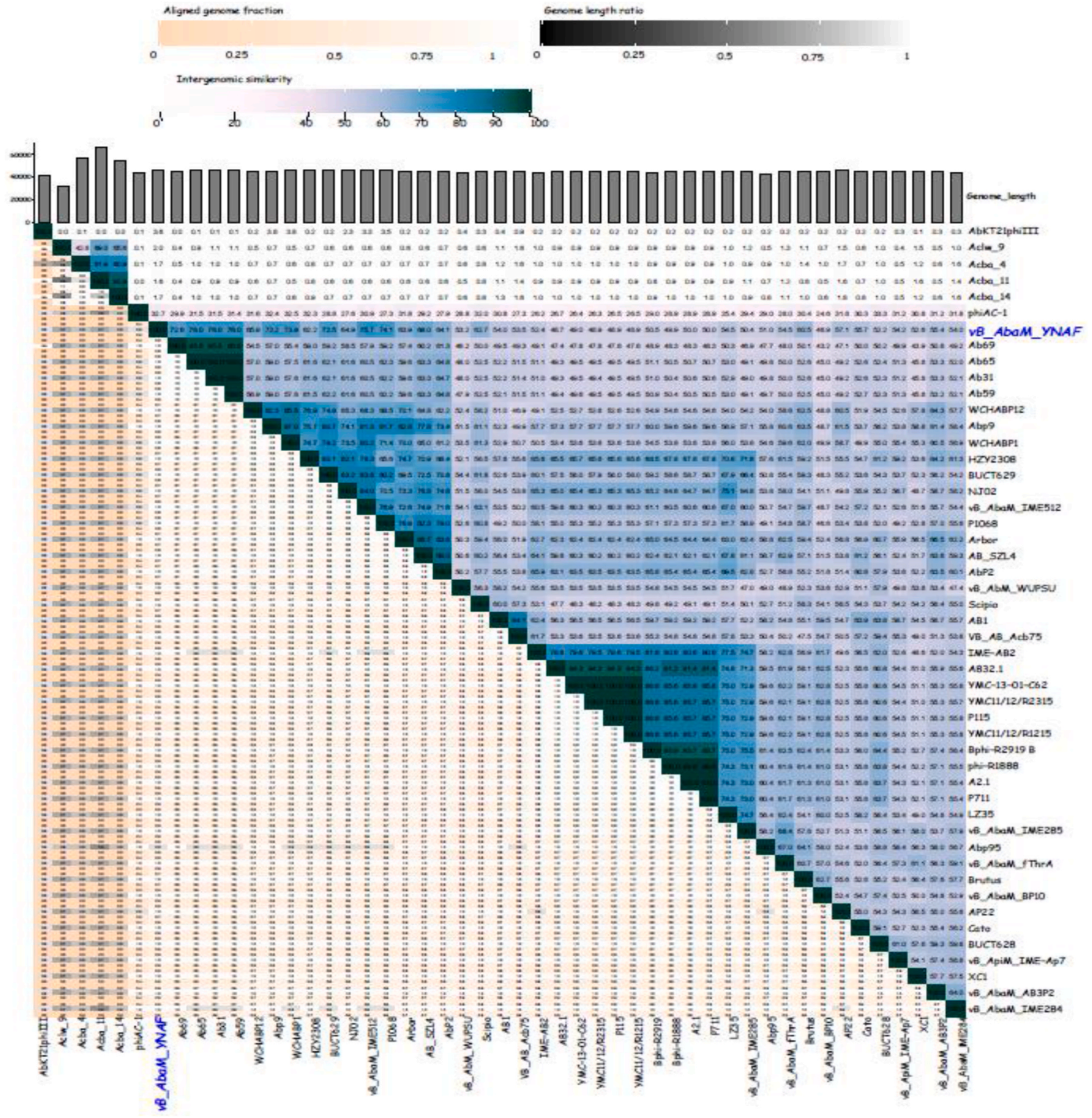

Fig. 8. Heatmap of phages genomically similar to vB_AbaM_YNAF.

Changes were seen in five different amino acids (I168V, S169K, E170S, G173E, and N176S) in the N terminus of the MazG protein. This may be attributed to the fact that phages of the same family follow different reproductive pathways. However, more study data on this subject is needed.

Endolysins are peptidoglycan-lytic enzymes that are synthesized by phages and are able to infect bacteria. During the phage's reproductive cycle, endolysins participate in the cleavage of peptidoglycan to release phage offspring. The higher bacterial selectivity and lower resistance risk suggest that lysins may be superior to antibiotics. However, the low antibiotic effects of lysins reported in research on Gram-negative bacteria are important limitations. Nonetheless, recent studies with outer membrane permeabilizers (OMPs), lysin combination trials, and engineered lysins are promising. Unlike lysins targeting Gram-positive bacteria, most lysins effective on Gram-negative bacteria have a broad host range and are active against different species.

The Gram-negative bacterial cell envelope is a complex structure composed of proteins, sugars, and intricate lipid arrangements [21]. Various strategies have been explored to enhance membrane permeability to lysins, including the co-administration of membrane-destabilizing agents such as poly-L-lysine, polymyxin B, and ethylenediaminetetraacetic acid disodium salt. Additionally, modifications to lysins themselves—such as the incorporation of highly charged or hydrophobic amino acid residues—have been investigated. However,

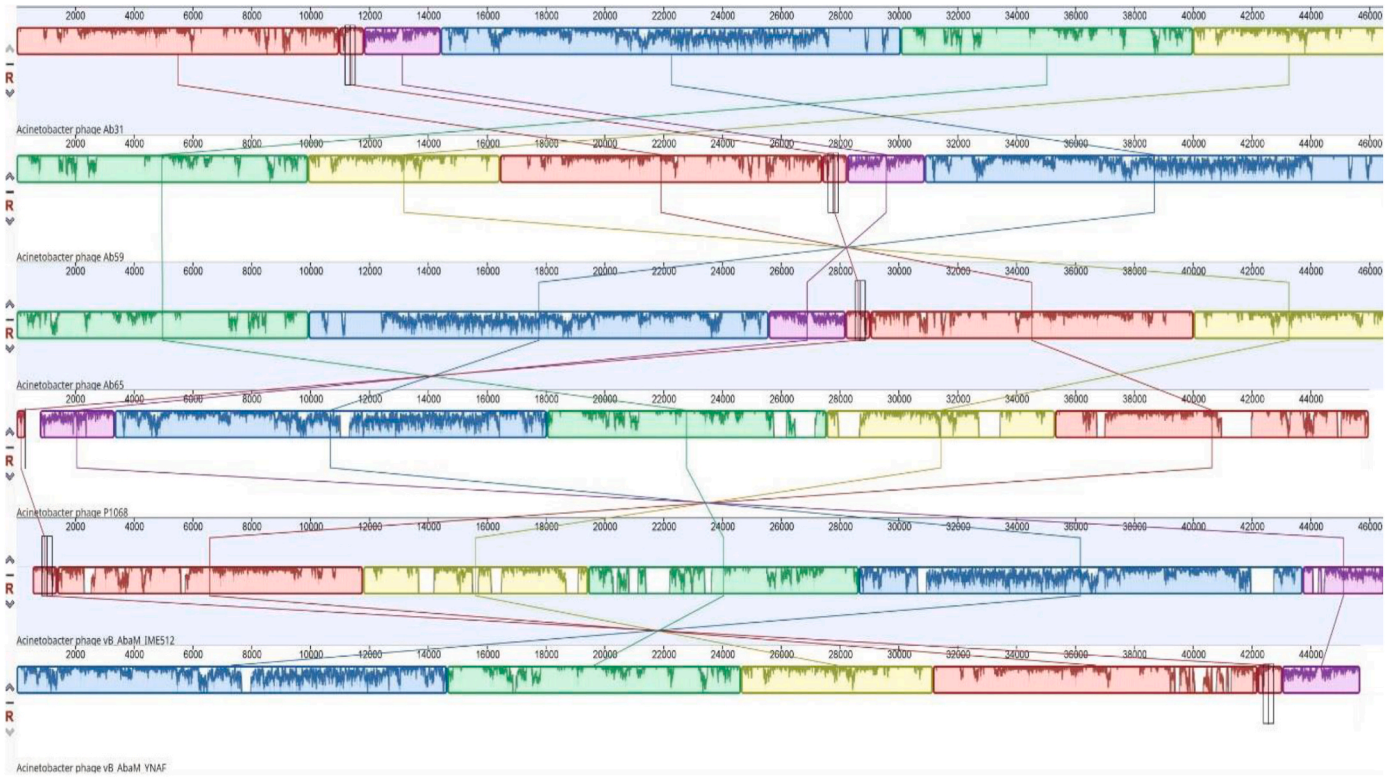

Fig. 9. Genomic comparison of vB_AbaM_YNAF genome with closest phage genomes.

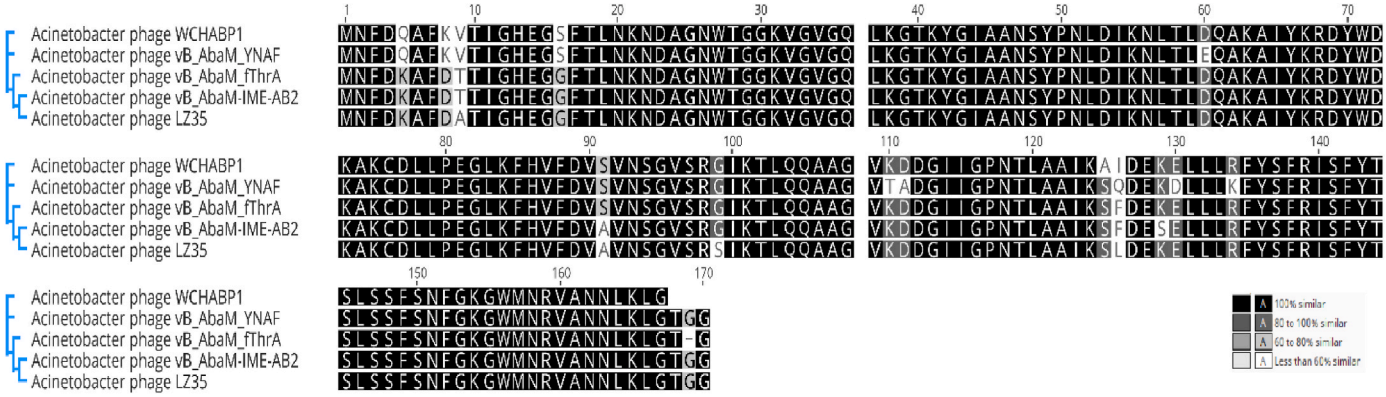

Fig. 10. Comparison of vB_AbaM_YNAF endolysin with closest endolysins.

Fig. 11. Comparison of vB_AbaM_YNAF holin and closest holins.

these approaches have yielded inconsistent results, with only a few demonstrating in vivo efficacy in animal models [22].

Physicochemical stability assessments conducted in vitro provide crucial insights into the development of effective phage therapies. While endolysin is expected to exhibit optimal activity under favorable conditions, its ability to function under extreme pH and temperature variations is a distinctive characteristic. Furthermore, stability profiles can vary across different phage families. A study on a *Siphoviridae* phage demonstrated optimal activity at pH 7 and 9, while losing viability at 70 °C [23]. In contrast, research on the *Acinetobacter* phage Abp9 from *Myoviridae* revealed that its endolysin remained active within a pH range of 6–10, with reduced activity beyond pH 12. Similar to vB_AbaM_YNAF, Abp9 lost its activity at pH 2 but exhibited stable performance between 20 °C and 60 °C [23]. In this study, the vB_AbaM_YNAF phage exhibited a similar stability profile to Abp9, showing no activity at pH 2 but maintaining stability between pH 4 and 12. Furthermore, it demonstrated optimal activity within a temperature range of 4 °C–50 °C, with a significant decline at 85 °C. These findings highlight the robustness of vB_AbaM_YNAF across diverse physicochemical conditions, underscoring its potential for therapeutic applications.

LysYNAF, a lysin specific to *A. baumannii*, was isolated from the *Acinetobacter* phage vB_AbaM_YNAF and shares sequence homology with both the glycoside hydrolase and muramidase/lysozyme-like superfamilies [24]. Unlike Gram-positive lysins, Gram-negative lysins such as LysYNAF typically consist of an N-terminal lysozyme-like domain and a C-terminal positively charged region [25]. The C-terminal region of LysYNAF is composed of basic amino acids that are thought to bind to the negatively charged lipopolysaccharides on the bacterial outer membrane. This binding is followed by the catalytic activity of the N-terminal domain, which cleaves the bonds between alternating N-acetylglucosamine and N-acetylmuramic acid residues in the bacterial peptidoglycan, leading to bacterial lysis [22].

Many studies have reported that only a few endolysins are active against *K. pneumoniae* due to the thick capsular polysaccharide layer in the outer cell wall [26,27]. Therefore, endolysins are more attractive than phage itself as an alternative antimicrobial agent for clinical treatment. However, due to the difficulties in quality control, studies are needed to evaluate phage as a real pharmaceutical [28].

We found that vB_AbaM_YNAF encodes an endolysin consisting of 170 amino acids and 108-glycosyl hydrolases. The enzyme exhibited a lytic effect on MDR *A. baumannii* and *K. pneumoniae*. Interestingly, the *Acinetobacter* phage WCHABP1 endolysin, which has the closest endolysin phylogenetically to the vB-AbaM_YNAF endolysin, has been shown to be from the glycoside hydrolase family, which hydrolyzes b-1,4-N-acetyl-D-glucosamine linkages in chitin polymers and can break chitin-containing cell walls [29]. vB_AbaM_YNAF endolysin is three amino acids longer than the WCHABP1 endolysin and contains seven amino acids (D60E, T110K, A111D, S125A, Q126I, D130E, and K134R). This functional difference can be associated with differences in the amino acid sequence.

Many DNA phages use holin-endolysin systems to release newly produced phages [30]. Holin contributes to endolysis, which reaches the periplasm to break down the peptidoglycan layer and make the cell membrane permeable by disrupting membrane proton flow [31,32]. Since most holins contain transmembrane domains, their coding genes are usually located around the genes encoding endolysin [31]. The holin of vB_AbaM_YNAF was not phylogenetically similar to the holin of the most closely related phages. On the contrary, it most closely resembled *Acinetobacter* phage Cato among the more distantly related bacteriophages. This suggests that differences in the endolysin-holin system may be responsible for the diversity of physiological effects of phages.

Bacteriophages can invade bacteria through lysozymes that cleave the β-1,4 glycosidic bonds of the cell membrane [33]. Lysozymes are also involved in the three-dimensional folding of proteins [34]. The lysozyme-containing protein may also be a part of the tail, as its base plate is close to the J-type protein. Lysozyme can be released from the inner tail tube to create a small hole in the peptidoglycan layer, permitting the phage genome to invade the cell [35]. The basal plate is the most distal part of the tail of the *Caudoviricetes*. It acts as a multi-protein molecular machine that binds to the host cell entry receptor, controls tail sheath contraction, and initiates genome expulsion. Genome expulsion is usually triggered by a change in baseplate conformation [36,37]. Zhou et al. [38] reported that *Acinetobacter* phage WCHABP1 and *Acinetobacter* phage WCHABP12 are effective against *A. baumannii*. *Acinetobacter* phage vB_AbaM_YNAF showed a lytic effect on *A. baumannii*. In addition, its lytic effect on different strains such as MDR *K. pneumoniae* may be associated with amino acid sequence differences.

Previous studies have highlighted the efficacy of phage therapy against MDR *A. baumannii*. For instance, a case report detailed the successful treatment of a patient with a MDR *A. baumannii* infection using a personalized phage therapy regimen [39]. Similarly, research has demonstrated the potential of phage therapy in managing *K. pneumoniae* infections, including strains resistant to multiple antibiotics [40]. These findings align with our results, underscoring the therapeutic promise of vB_AbaM_YNAF.

Our study adds to this growing body of evidence by demonstrating that vB_AbaM_YNAF exhibits a broad host range and strong lytic activity against MDR Gran-negative strains. This contrasts with previous reports where some phages showed a narrow host range, highlighting the unique potential of vB_AbaM_YNAF [41,42].

5. Conclusion

In this article, we isolated and characterized a novel bacteriophage of novel origin that can infect reference and MDR *A. baumannii* and *K. Pneumoniae* strains. The bacteriophage acted to inhibit MDR *A. baumannii* and *K. pneumoniae*. This broad host range suggests potential therapeutic applications for vB_AbaM_YNAF in treating infections caused by these pathogens. Bioinformatics and phylogenetic analyses showed that the phage represents a new species of unclassified *Obolenskvirus* within *Caudoviricetes*. Notably, phage therapy offers specificity in targeting pathogenic bacteria while sparing the beneficial microbiota, reducing the likelihood of dysbiosis. In conclusion, vB_AbaM_YNAF exhibits significant potential as a therapeutic agent against MDR *A. baumannii* and *K. pneumoniae* infections. Its broad host range, coupled with its unique genomic characteristics, positions it as a strong candidate for phage therapy applications. Future in vivo studies and clinical trials are warranted to assess its safety, efficacy, and potential integration into existing treatment protocols.

CRediT authorship contribution statement

Yelda İşlek: Writing – original draft, Methodology. **Nur Hamzeli:** Writing – original draft, Methodology, Investigation. **Ahmet Aktaş:** Writing – review & editing, Writing – original draft, Visualization, Software, Methodology, Formal analysis. **Fatma Köksal Çakırlar:** Project administration.

Ethical approval

Not required.

Sequence information

GenBank database under the accession number PP355976.

Declaration of competing interest

The authors declare that they have no known competing financial interests or personal relationships that could have appeared to influence the work reported in this paper.

Data availability

Data will be made available on request.

References

[1] A. Howard, M. O'Donoghue, A. Feeney, R.D. Sleator, Acinetobacter baumannii: an emerging opportunistic pathogen, Virulence 3 (3) (2012) 243–250, https://doi.org/10.4161/viru.19700.

[2] O. Ayobami, N. Willrich, B. Suwono, T. Eckmanns, R. Markwart, The epidemiology of carbapenem-non-susceptible Acinetobacter species in Europe: analysis of EARS-Net data from 2013 to 2017, Antimicrob. Resist. Infect. Control 9 (1) (2020) 89, https://doi.org/10.1186/s13756-020-00750-5.

[3] S. Roy, G. Chowdhury, A.K. Mukhopadhyay, S. Dutta, S. Basu, Convergence of biofilm formation and antibiotic resistance in Acinetobacter baumannii infection, Front. Med. 9 (2022) 793615, https://doi.org/10.3389/fmed.2022.793615.

[4] G.V. Asokan, T. Ramadhan, E. Ahmed, H. Sanad, WHO Global Priority Pathogens List: a bibliometric analysis of Medline-PubMed for knowledge mobilization to infection prevention and control practices in Bahrain, Oman Med. J. 34 (3) (2019) 184–193, https://doi.org/10.5001/omj.2019.37.

[5] Z. Naureen, A. Dautaj, K. Anpilogov, G. Camilleri, K. Dhuli, B. Tanzi, et al., Bacteriophages presence in nature and their role in the natural selection of bacterial populations, Acta Biomed. 91 (13-S) (2020) e2020024, https://doi.org/10.23750/abm.v91i13-S.10819.

[6] D.E. Fruciano, S. Bourne, Phage as an antimicrobial agent: d'Herelle's heretical theories and their role in the decline of phage prophylaxis in the West, Can. J. Infect. Dis. Med. Microbiol. 18 (1) (2007) 19–26, https://doi.org/10.1155/2007/976850.

[7] J. Taslem Mourosi, A. Awe, W. Guo, H. Batra, H. Ganesh, X. Wu, et al., Understanding bacteriophage tail fiber interaction with host surface receptor: the key "blueprint" for reprogramming phage host range, Int. J. Mol. Sci. 23 (20) (2022) 12146, https://doi.org/10.3390/ijms232012146.

[8] L.M. Kasman, L.D. Porter, Bacteriophages. https://pubmed.ncbi.nlm.nih.gov/29630237/, 2022.

[9] M. Merabishvili, D. Vandenheuvel, A.M. Kropinski, J. Mast, D. De Vos, G. Verbeken, et al., Characterization of newly isolated lytic bacteriophages active against Acinetobacter baumannii, PLoS One 9 (8) (2014) e104853, https://doi.org/10.1371/journal.pone.0104853.

[10] X. Liang, Y. Wang, B. Hong, Y. Li, Y. Ma, J. Wang, Isolation and characterization of a lytic Vibrio parahaemolyticus phage VB_VpaP_GHSM17 from sewage samples, Viruses 14 (2022) 1601.

[11] A.S. Abdelsattar, M.A. Eita, Z.K. Hammouda, S.M. Gouda, T.A. Hakim, A. Y. Yakoup, et al., The lytic activity of bacteriophage ZCSE9 against *Salmonella enterica* and its synergistic effects with kanamycin, Viruses 15 (2023) 912.

[12] Z. Wang, P. Zheng, W. Ji, Q. Fu, H. Wang, Y. Yan, et al., SLPW: a virulent bacteriophage targeting methicillin-resistant *Staphylococcus aureus* in vitro and in vivo, Front. Microbiol. 7 (2016) 934.

[13] D. Nabergoj, P. Modic, A. Podgornik, Effect of bacterial growth rate on bacteriophage population growth rate, Microbiol. 7 (2) (2018) e00558.

[14] O.A. Taha, P.L. Connerton, I.F. Connerton, A. El-Shibiny, Bacteriophage ZCKP1: a potential treatment for *Klebsiella pneumoniae* isolated from diabetic foot patients, Front. Microbiol. 9 (2018) 2127.

[15] S. Santajit, N. Indrawattana, Mechanisms of antimicrobial resistance in ESKAPE pathogens, BioMed Res. Int. 2016 (2016) 2475067, https://doi.org/10.1155/2016/2475067.

[16] N.D. Menon, M.S. Kumar, T.G. Satheesh Babu, S. Bose, G. Vijayakumar, M. Baswe, et al., A novel N4-like bacteriophage isolated from a wastewater source in South India with activity against several multidrug-resistant clinical *Pseudomonas aeruginosa* isolates, mSphere 6 (1) (2021) e01215, https://doi.org/10.1128/mSphere.01215-20, 20.

[17] S. Kanamaru, K. Kondabagil, M.G. Rossmann, V.B. Rao, The functional domains of bacteriophage T4 terminase, J. Biol. Chem. 279 (39) (2004) 40795–40801, https://doi.org/10.1074/jbc.M403647200.

[18] C.R. Büttner, M. Chechik, M. Ortiz-Lombardía, C. Smits, I.O. Ebong, V. Chechik, et al., Structural basis for DNA recognition and loading into a viral packaging motor, Proc. Natl. Acad. Sci. U. S. A. 109 (3) (2012) 811–816, https://doi.org/10.1073/pnas.1110270109.

[19] M.G. Rossmann, Structure of viruses: a short history, Q. Rev. Biophys. 46 (2) (2013) 133–180, https://doi.org/10.1017/S0033583513000012.

[20] M.J. Bryan, N.J. Burroughs, E.M. Spence, M.R. Clokie, N.H. Mann, S.J. Bryan, Evidence for the intense exchange of MazG in marine cyanophages by horizontal gene transfer, PLoS One 3 (4) (2008) e2048, https://doi.org/10.1371/journal.pone.0002048.

[21] L.L. Silver, A gestalt approach to Gram-negative entry, Bioorg. Med. Chem. 24 (2016) 6379–6389, https://doi.org/10.1016/j.bmc.2016.06.044.

[22] C. Ghose, C.W. Euler, Gram-negative bacterial lysins, Antibiotics (Basel) 9 (2) (2020) 74, https://doi.org/10.3390/antibiotics9020074.

[23] M. Mardiana, S.H. Teh, L.C. Lin, N.T. Lin, Isolation and characterization of a novel Siphoviridae phage, vB_AbaS_TCUP2199, infecting multidrug-resistant Acinetobacter baumannii, Viruses 14 (2022) 1240, https://doi.org/10.3390/v14061240.

[24] L. Jiang, J. Tan, Y. Hao, Q. Wang, X. Yan, D. Wang, L. Tuo, Z. Wei, G. Huang, Isolation and characterization of a novel myophage Abp9 against pandrug-resistant Acinetobacter baumannii, Front. Microbiol. 11 (2020) 506068, https://doi.org/10.3389/fmicb.2020.506068.

[25] M.J. Lai, N.T. Lin, A. Hu, P.C. Soo, L.K. Chen, L.H. Chen, K.C. Chang, Antibacterial activity of Acinetobacter baumannii phage varphiAB2 endolysin (LysAB2) against both Gram-positive and Gram-negative bacteria, Appl. Microbiol. Biotechnol. 90 (2011) 529–539, https://doi.org/10.1007/s00253-011-3104-y.

[26] R. Vázquez, E. García, P. García, Phage lysins for fighting bacterial respiratory infections: a new generation of antimicrobials, Front. Immunol. 9 (2018 Oct 16) 2252, https://doi.org/10.3389/fimmu.2018.02252.

[27] U. Sharma, A. Vipra, S. Channabasappa, Phage-derived lysins as potential agents for eradicating biofilms and persisters, Drug Discov. Today 23 (4) (2018 Apr) 848–856, https://doi.org/10.1016/j.drudis.2018.01.026.

[28] X. Zhen, C.S. Lundborg, X. Sun, X. Hu, H. Dong, Economic burden of antibiotic resistance in ESKAPE organisms: a systematic review, Antimicrob. Resist. Infect. Control 8 (2019 Aug 13) 137, https://doi.org/10.1186/s13756-019-0590-7.

[29] S. Kim, D.W. Lee, J.S. Jin, J. Kim, Antimicrobial activity of LysSS, a novel phage endolysin, against Acinetobacter baumannii and Pseudomonas aeruginosa, J Glob Antimicrob Resist 22 (2020 Sep) 32–39, https://doi.org/10.1016/j.jgar.2020.01.005.

[30] M.J. Lai, K.C. Chang, S.W. Huang, C.H. Luo, P.Y. Chiou, C.C. Wu, et al., The tail associated protein of acinetobacter baumannii phage ΦAB6 is the host specificity determinant possessing exopolysaccharide depolymerase activity, PLoS One 11 (4) (2016 Apr 14) e0153361, https://doi.org/10.1371/journal.pone.0153361.

[31] I. Young, I. Wang, W.D. Roof, Phages will out: strategies of host cell lysis, Trends Microbiol. 8 (3) (2000 Mar) 120–128, https://doi.org/10.1016/s0966-842x(00)01705-4.

[32] R.S. Pollenz, J. Bland, W.H. Pope, Bioinformatic characterization of endolysins and holin-like membrane proteins in the lysis cassette of phages that infect Gordonia rubripertincta, PLoS One 17 (11) (2022 Nov 17) e0276603, https://doi.org/10.1371/journal.pone.0276603.

[33] J. Pei, N.V. Grishin, COG3926 and COG5526: a tale of two new lysozyme-like protein families, Protein Sci. 14 (10) (2005 Oct) 2574–2581, https://doi.org/10.1110/ps.051656805.

[34] G. Merlini, V. Bellotti, Lysozyme: a paradigmatic molecule for the investigation of protein structure, function and misfolding, Clin. Chim. Acta 357 (2) (2005 Jul 24) 168–172, https://doi.org/10.1016/j.cccn.2005.03.022.

[35] R.L. Duda, Icosahedral tailed dsDNA bacterial viruses, in: Brian W.J. Mahy, Marc H.V. Van Regenmortel (Eds.), Encyclopedia of Virology, third ed., Academic Press, 2008, pp. 30–37. ISBN 9780123744104.

[36] M.G. Rossmann, V.V. Mesyanzhinov, F. Arisaka, P.G. Leiman, The bacteriophage T4 DNA injection machine, Curr. Opin. Struct. Biol. 14 (2) (2004 Apr) 171–180, https://doi.org/10.1016/j.sbi.2004.02.001.

[37] G. Sciara, C. Bebeacua, P. Bron, D. Tremblay, M. Ortiz-Lombardia, J. Lichière, et al., Structure of lactococcal phage p2 baseplate and its mechanism of activation, Proc. Natl. Acad. Sci. U. S. A. 107 (15) (2010 Apr 13) 6852–6857, https://doi.org/10.1073/pnas.1000232107.

[38] W. Zhou, Y. Feng, Z. Zong, Two new lytic bacteriophages of the Myoviridae family against carbapenem-resistant acinetobacter baumannii, Front. Microbiol. 9 (2018 Apr 30) 850, https://doi.org/10.3389/fmicb.2018.00850.

[39] R.T. Schooley, B. Biswas, J.J. Gill, A. Hernandez-Morales, J. Lancaster, L. Lessor, et al., Development and use of personalized bacteriophage-based therapeutic cocktails to treat a patient with a disseminated resistant acinetobacter baumannii infection, Antimicrob. Agents Chemother. 61 (10) (2017 Sep 22) e00954, 17. doi: 10.1128/AAC.00954-17. Erratum in: Antimicrob Agents Chemother. 2018 Nov 26; 62(12):e02221-18. doi: 10.1128/AAC.02221-18.

[40] S. Chhibber, S. Kaur, S. Kumari, Therapeutic potential of bacteriophage in treating Klebsiella pneumoniae B5055-mediated lobar pneumonia in mice, J. Med. Microbiol. 57 (Pt 12) (2008 Dec) 1508–1513, https://doi.org/10.1099/jmm.0.2008/002873-0.

[41] L. Jiang, J. Tan, Y. Hao, Q. Wang, X. Yan, D. Wang, et al., Isolation and characterization of a novel myophage Abp9 against pandrug resistant acinetobacater baumannii, Front. Microbiol. 11 (2020 Sep 8) 506068, https://doi.org/10.3389/fmicb.2020.506068. Erratum in: Front Microbiol. 2020 Dec 03;11: 625283. doi: 10.3389/fmicb.2020.625283.

[42] J.J.K. Chu, W.H. Poh, N.T.B. Hasnuddin, E.Y. Hew, L.C. Dam, A.E. Sahili, S.A. Rice, B.C. Goh, Novel Phage Lysin Abp013 against Acinetobacter baumannii. Antibiotics (Basel) 11 (2) (2022 Jan 28) 169, https://doi.org/10.3390/antibiotics11020169.